

## DESCRIPTION OF THE NORTHEASTERN PACIFIC OCEANOGRAPHY

NICHOLAS P. FOFONOFF

Before coming here I went around our building at Nanaimo and gathered a few drawings from people who had worked on various things that had happened in the ocean in 1957, to see if, and how, they differed from previous years. The figures are samples of the type of data that has been collected.

Figure 85 shows the variation of surface temperatures along the coast. Daily observations of temperature and salinity are made at lighthouse stations at various parts of the British Columbia Coast. About fourteen stations are currently sending in these observations. Two of these stations along the outer coast have been selected to contrast temperatures in 1956 and 1957. Both show that 1957 temperatures were higher and that 1956 temperatures were lower than the ten year average.

The surface temperatures at Amphitrite Point on Vancouver Island began to increase in March and at Langara Island, just off the northern end of the Queen Charlotte Islands in April of 1957. Temperatures at both locations continued to be above average throughout the winter of 1957.

The solid curves in figure 85 are monthly mean and the broken curves the mean over the preceding ten

years. Figure 86 is based on observations taken at Ocean Station "Papa," located at 50°N, 145°W. Oceanographic observations are taken here in alternate six-week periods throughout the year. These observations, apart from BT's, were started in 1956 and are continuing at present. Twice-daily BT's are available from 1952.

The largest fluctuations of salinity occur in the upper part of the halocline (maximum in autumn, minimum in spring). The salinity has gradually increased in the upper part of the halocline (75-150m) and decreased in the lower part. For example, from August 1956 to January 1958 the salinity at 200 meters decreased by 0.20‰. The trend is shown in the T-S curves for the weathership data in figure 86. Each curve is the mean over a six-week period. The seasonal temperature variation is limited to the upper 50 meters. Below this depth, fluctuations are not clearly related to the seasonal cycle. A gradual warming has been observed in the upper part of the halocline. For example, the temperature at 125 meters has increased by 1.5°C. This trend is still continuing. An indication of the temperature change is given in figure 87 in which a comparison is made of the temperature at the surface and 70 meters (200 feet) in

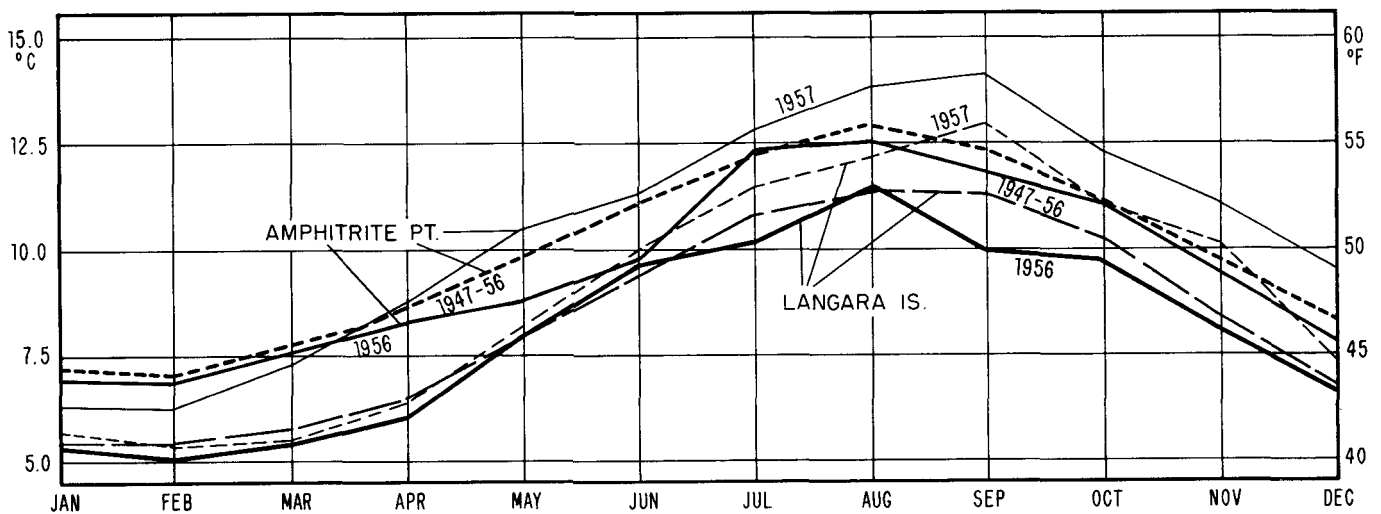


FIGURE 85. Mean monthly seawater temperatures during 1956 and 1957 compared with grand monthly mean at Langara Island and Amphitrite Point. Reference: Observations of seawater temperature and salinity on the Pacific Coast of Canada. MSS Report, Fish. Res. Bd. Can. Vol. XVI, 1956, Vol. XVII, 1957.

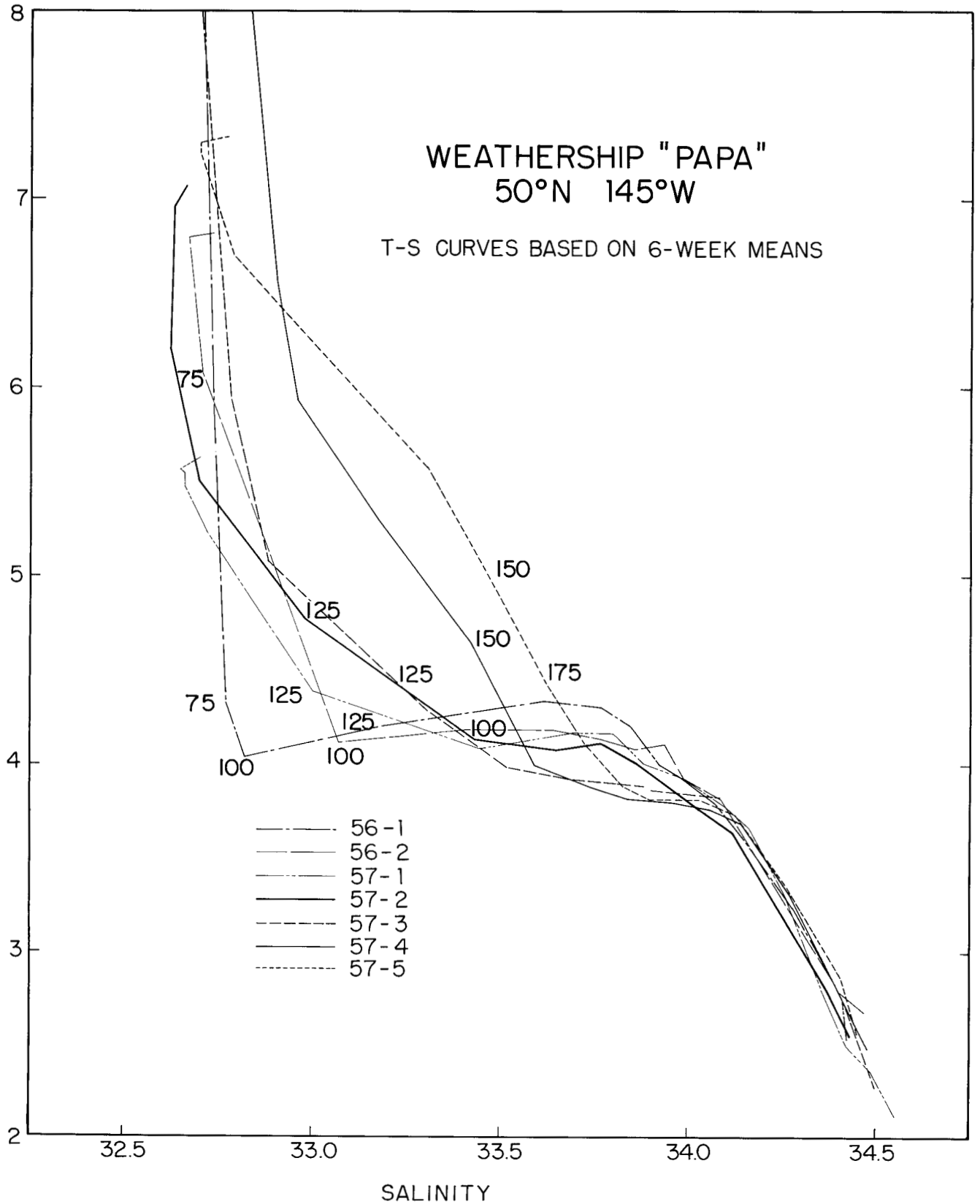


FIGURE 86. Temperature-Salinity relationships based on means of alternate six-week periods at Weathership "Papa" 50°N 145°W, after S. Tabata.

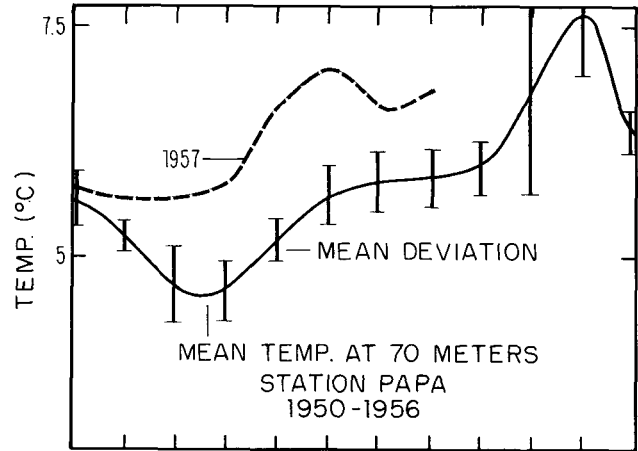
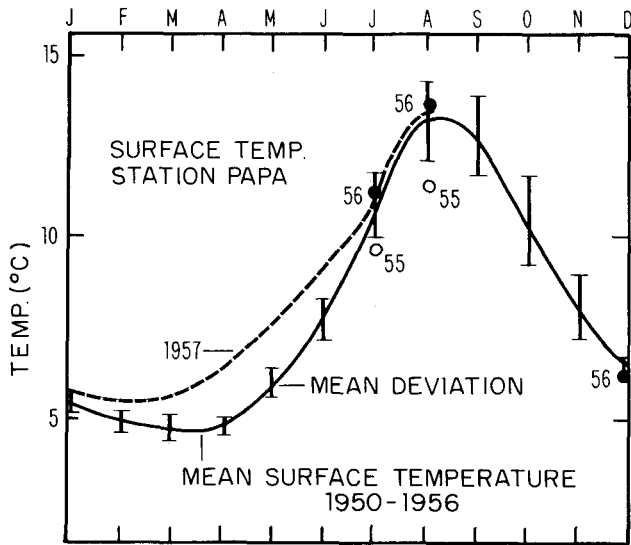


FIGURE 87. Surface and 70 meter temperatures in 1957 compared with the 1950-1956 mean at Weathership "Papa", after S. Tabata.

1957 with the mean for 1950 to 1956. The temperatures in 1957 were substantially higher at 70 meters as compared with the previous seven year period.

The oxygen has been steadily increasing in and below the halocline. An increase of 0.2 mg.at./l has been observed in the depth interval 150 to 300 meters.

Drift bottle studies were initiated in August 1956 and will continue to at least August 1958. Bottles were dropped in lots of 1000 each periodically from the weatherships (Fig. 88) and during NORPAC cruises (Fig. 89). So far, about 25,000 bottles have been released with 816 recoveries to the middle of April 1958. Returns varied from 0 to 16% for individual releases with an overall average of 3.3%. The time at sea varied from four months to one year.

The distribution of returns suggests that shifts in the surface current system occur. The northward component of the current between the weathership and the coast appeared to strengthen after September 1956, weaken in January 1957 and strengthen again in March to July 1957. The stronger northward flow in the summer of 1957 is also suggested by the dynamic topography.

The most southerly releases 40°N to 42°N did not reach the coast (one bottle was picked up on the Hawaiian Islands).

Speeds of drift ranged from 3 to 9 miles per day (6-19 cm/sec) somewhat higher than computed surface geostrophic velocities.

The region near the coast of British Columbia has been surveyed quite intensively in the last two years. The analysis is not completed but there is evidence for marked variations in the northward flow of warm saline water. During 1957 the volume of northward flow appeared to be larger although the temperatures were not significantly higher.

### COMMENTS ON THE WIND-DRIVEN OCEAN CIRCULATION

In the interior of the ocean away from the direct influence of coastal boundaries, the steady-state currents are assumed to satisfy a simple set of equations of the form:

$$-\rho f v = -\frac{\partial p}{\partial x} + \frac{\partial \tau_x}{\partial z} \tag{1}$$

$$\rho f u = -\frac{\partial p}{\partial y} + \frac{\partial \tau_y}{\partial z} \tag{2}$$

$$\frac{\partial \rho u}{\partial x} = \frac{\partial \rho v}{\partial y} + \frac{\partial \rho w}{\partial z} = 0 \tag{3}$$

We can split up the velocity vector  $\mathbf{V}$  into two parts so that

$$\mathbf{V} = \mathbf{V}_g + \mathbf{V}_w \tag{4}$$

where  $\mathbf{V}_g$  is geostrophic velocity and  $\mathbf{V}_w$  is wind drift. The equations then become

$$\left. \begin{aligned} -f \mathbf{V}_g &= -\frac{\partial p}{\partial x} \\ f u_g &= -\frac{\partial p}{\partial y} \end{aligned} \right\} \begin{array}{l} \text{Geostrophic} \\ \text{"observed"} \end{array} \tag{5}$$

$$\left. \begin{aligned} -f \mathbf{V}_w &= \frac{\partial \tau_x}{\partial z} \\ f u_w &= \frac{\partial \tau_y}{\partial z} \end{aligned} \right\} \begin{array}{l} \text{Ekman Spiral Equations} \\ \text{"Shallow nongeostrophic currents"} \end{array} \tag{6}$$

and

$$\text{div } \rho \mathbf{V}_g + \text{div } \rho \mathbf{V}_w + \frac{\partial \rho w}{\partial z} = 0 \tag{7}$$

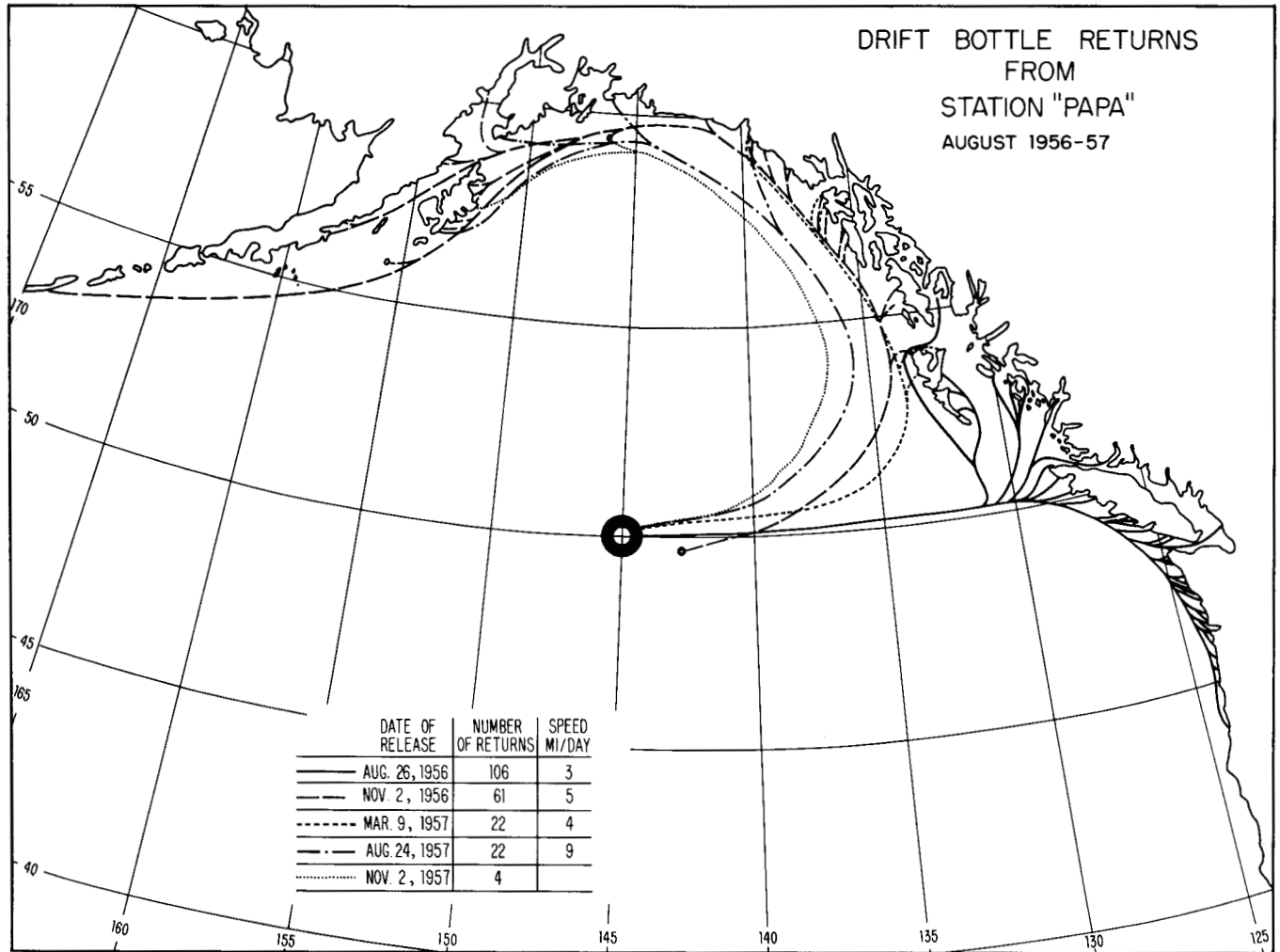


FIGURE 88. Drift bottle returns from WeatherShip "Papa." Reference: A. J. Dodimead and H. J. Hollister 1958: Progress Report of drift bottles releases in the Northeast Pacific Ocean. *Jour. Fish. Res. Bd. Can.* 15 (5), pp. 851-865.

Where  $\text{div } \rho \mathbf{V}$  refers to divergence of horizontal components only.

Taking the curl of the momentum equations yields

$$f \text{div } \rho \mathbf{V}_\theta + \beta \mathbf{V}_\theta = 0 \tag{8}$$

$$f \text{div } \rho \mathbf{V}_w + \beta \mathbf{V}_w = \frac{\partial}{\partial z} \text{curl}_z \tau \tag{9}$$

The wind drift according to the Ekman Theory is confined to the upper layers (~ upper 100 meters) whereas the geostrophic currents can extend much deeper. It is therefore evident from (8) that if the geostrophic current has a meridional component there will be a horizontal divergence over most of the depth as required to conserve absolute vorticity. The surface wind stress would add or remove vorticity from the wind drift currents only.

Equations (8) and (9) can be added and integrated vertically to yield the familiar result

$$-f(w_s - w_b) + \beta \int v dz + \text{curl}_z \tau, \tag{10}$$

which, if we neglect the vertical motion  $w$ , is the result obtained by Munk (1950). If the  $\text{curl}_z \tau$  is zero, the total transport is zero. This is interpreted to mean that the transport of the wind drift is equal and opposite to the geostrophic transport. However, since the geostrophic currents can extend to much greater depths than the wind drift currents, the resulting circulation can be quite effective in transporting heat and salt.

The wind drift is always directed to the right of the wind in the Northern Hemisphere, but the geostrophic

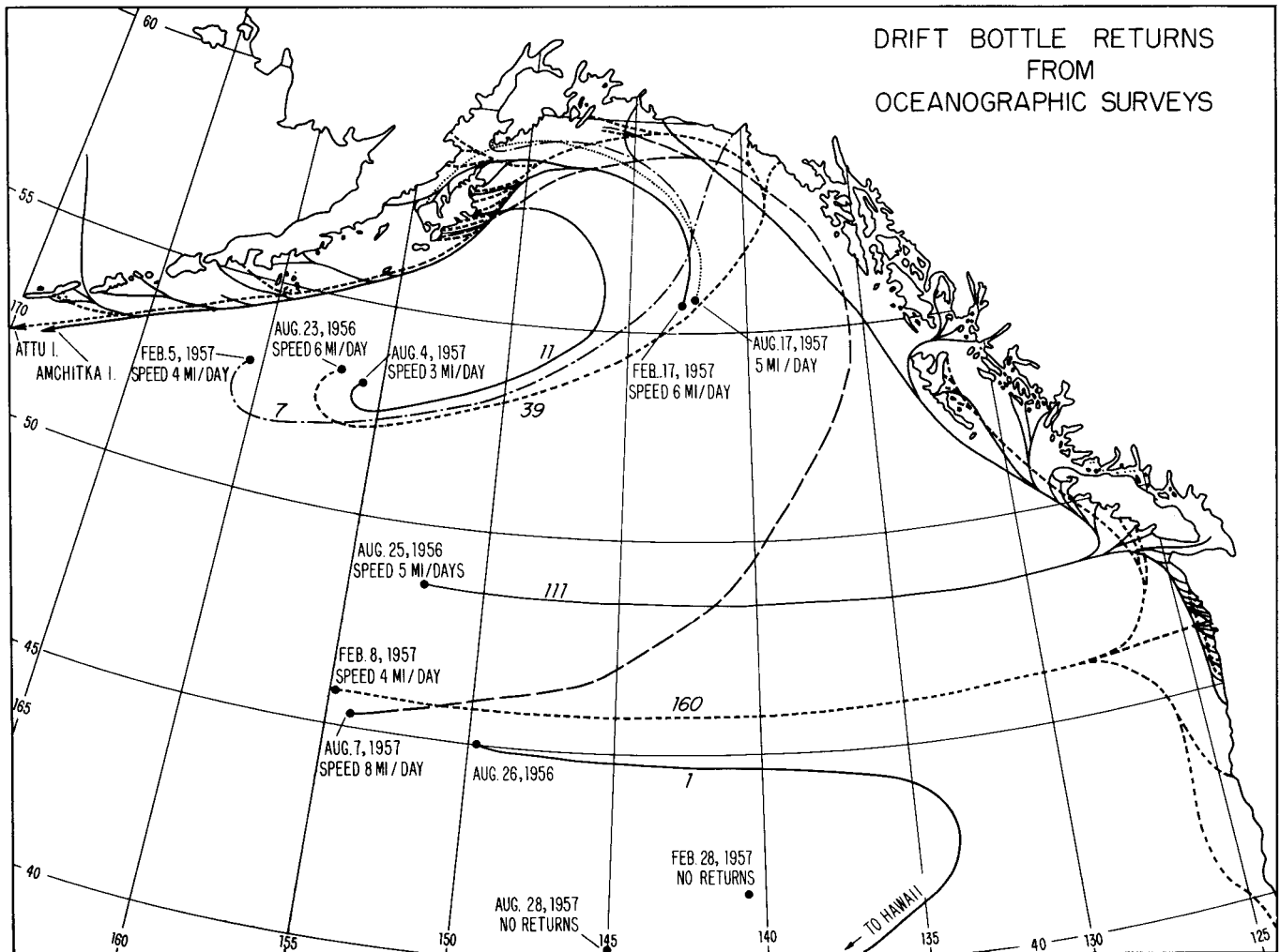


FIGURE 89. Drift bottle returns from NORPAC Cruises. Reference: A. J. Dodimead and H. J. Hollister 1958: Progress Report of drift bottles releases in the Northeast Pacific Ocean. *Jour. Fish. Res. Bd. Can.* 15 (5), pp. 851-865.

current can be to the right, left or against the wind depending on the stress distribution over the surface. Hence, it is often difficult to correlate dynamic topography to the wind system. Conversely, the dynamic topography would not be an entirely reliable guide to surface currents if the geostrophic velocities are of the same magnitude or smaller than the wind drift currents.

### DEEP CURRENTS

Munk's analysis of wind-driven ocean circulation depends critically on the assumption of zero pressure gradient in the lower layers. We see from equation (10), neglecting  $w_s$  at the surface, that

$$fw_b + \beta \int v dz = \text{curl}_z \tau \quad (11)$$

If  $\text{curl}_z \tau$  is of the order of  $10^{-8}$  dynes/cm<sup>3</sup>, a vertical velocity of  $10^{-4}$  cm/sec would be enough to seriously influence the conclusions of Munk's theory. The vertical velocities required to satisfy vorticity conservation are of this order of magnitude.

The divergence in each layer of the geostrophic flow will produce a pressure gradient in the layers beneath it. Consequently, the geostrophic flow cannot be uniform and the current vector must veer to the right or left with depth depending on the motion in the deep water. It is, in fact, possible to construct a deep current system which exactly compensates the divergence of the upper geostrophic currents. Such a current system could then persist for a long time in the absence of surface winds.

